

Original Article

### Development and Optimization of Danazol Co-crystal loaded tablet to treat endometriosis

Vidya Patil<sup>\*1</sup>, Shivraj Jadhav<sup>1</sup>, Sunil Mahajan<sup>2</sup>

<sup>1</sup> Department of Pharmaceutics, Divine College of Pharmacy, Nashik, Maharashtra, India 422301.

<sup>2</sup> Department of pharmaceutical chemistry, Divine College of Pharmacy, Nashik, Maharashtra, India 422301.

\* Correspondence, e-mail: vidyapatil03112001@gmail.com

Received: 25.05.2025 / Revised: 21.07.2025 / Accepted: 06.08.2025 / Published online: 01.10.2025

#### ABSTRACT

**Objectives:** To develop, optimize, and characterize danazol co-crystal-loaded tablets for enhanced solubility and dissolution to improve therapeutic efficacy in endometriosis treatment. **Methods:** Danazol co-crystals were prepared using various co-formers through solvent evaporation technique and characterized by FTIR, DSC, and XRD. Co-crystals were formulated into tablets using direct compression and optimized through 3<sup>2</sup> factorial design, varying sodium croscarmellose (8-24 mg) and PVP K-30 (4-20 mg) concentrations. Formulations were evaluated for pre-compression properties, physical parameters, disintegration, dissolution, and stability. **Results:** Danazol-malonic acid co-crystals (1:2 ratio) exhibited the highest solubility enhancement ( $11.42 \pm 0.53 \mu\text{g/mL}$ , 13.76-fold increase). XRD confirmed the formation of a new crystalline phase with distinct peaks at  $19^\circ$  and  $21^\circ$   $2\theta$ . The quadratic models for both disintegration time ( $R^2 = 0.9971$ ) and drug release ( $R^2 = 0.9483$ ) demonstrated excellent predictive capability. Formulation VF7 (24 mg sodium croscarmellose, 4 mg PVP K-30) was identified as optimal with rapid disintegration ( $74.0 \pm 3.2$  seconds) and superior dissolution ( $83.6 \pm 3.4\%$  at 30 minutes,  $95.8 \pm 2.0\%$  at 60 minutes) compared to the marketed product ( $75.2 \pm 2.7\%$  at 60 minutes). The optimized formulation-maintained stability under accelerated conditions ( $40^\circ\text{C}/75\% \text{RH}$ ) for three months. **Conclusion:** The optimized Danazol co-crystal tablet formulation successfully overcame the solubility and dissolution limitations of this poorly soluble drug, potentially enhancing bioavailability and therapeutic efficacy while reducing dosing frequency for endometriosis patients. This approach presents a promising platform for improving clinical outcomes and patient compliance in endometriosis management.

**KEYWORDS:** Danazol, Co-crystallization, Solubility enhancement, Factorial design, Endometriosis, Bioavailability

Article is published under the CC BY license.

#### 1. INTRODUCTION

Endometriosis affects approximately 10% of reproductive-aged women globally, affecting an estimated 190 million individuals worldwide [1]. This chronic inflammatory condition, characterized by the growth of endometrial tissue outside the uterine cavity, imposes a substantial economic burden of \$69-119 billion annually in the United States alone through direct healthcare costs and lost productivity [2]. Current pharmaceutical interventions primarily consist of hormonal therapies and analgesics that provide symptomatic relief rather than disease modification, with up to 50% of patients experiencing treatment failure or intolerable side effects [3]. The disease significantly diminishes quality of life, with 38% of patients reporting reduced work productivity and 11% experiencing complete work disability [2]. Despite recent advances in minimally invasive surgical techniques,

recurrence rates remain high at 40-50% within five years post-operation [4]. The persistent challenges in effectively managing endometriosis highlight the urgent need for novel therapeutic approaches with improved efficacy and tolerability profiles [5].

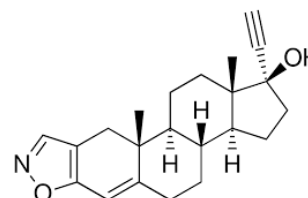


Fig. 1: Chemical structure of Danazol

Danazol, a synthetic androgen derivative (Fig.1) (17 $\alpha$ -ethynyl testosterone), represents a potentially valuable therapeutic agent for endometriosis due to its multimodal

mechanism of action [6,7]. The compound exhibits a molecular weight of 337.46 g/mol and demonstrates moderate lipophilicity ( $\log P = 4.53$ ), aqueous solubility values ranging from 0.4-0.6  $\mu\text{g/mL}$  under standard conditions, with variations up to 10-18  $\mu\text{g/mL}$  depending on experimental conditions, temperature, and analytical methods employed. Structurally characterized by a modified steroid nucleus with an ethynyl group at C-17 and a 2,3-isoxazole ring, danazol exerts its therapeutic effects through inhibition of pituitary gonadotropin secretion, direct suppression of endometrial tissue growth, and modulation of inflammatory pathways [8]. Clinical studies have demonstrated efficacy rates of 60-90% for pain reduction and endometriotic lesion regression. However, conventional danazol formulations require high doses (400-800 mg daily) to achieve therapeutic plasma concentrations, often resulting in androgenic side effects that limit patient compliance and clinical utility [9]. Recent investigations into structural modifications and alternative delivery systems present promising opportunities to revitalize this established compound for improved endometriosis management [10].

The co-crystallization approach represents an innovative strategy to overcome the pharmaceutical limitations of danazol through the formation of supramolecular structures with complementary co-formers [11]. This technology exploits non-covalent interactions predominantly hydrogen bonding,  $\pi$ - $\pi$  stacking, and van der Waals forces to create crystalline lattices with enhanced physicochemical properties [12]. Co-crystallization of danazol with selected GRAS (Generally Recognized as Safe) compounds has demonstrated substantial improvements in aqueous solubility (up to 12-fold increase) and dissolution rates (5-fold enhancement) in preliminary investigations [13]. The tablet delivery system incorporating these co-crystals employs modified release technology to optimize pharmacokinetic parameters and reduce dosing frequency. Recent advances in pharmaceutical engineering have demonstrated various approaches for co-crystal formation and formulation, with solvent evaporation techniques showing particular promise for laboratory-scale development and characterization studies. This approach potentially addresses multiple challenges simultaneously: improving bioavailability, reducing required doses, minimizing side effects, and enhancing patient adherence for endometriosis management [14].

The present study aims to develop, characterize, and optimize danazol co-crystal loaded tablets specifically designed for endometriosis treatment. The research will evaluate various co-formers for optimal physicochemical enhancement, establish robust manufacturing processes, and assess in vitro performance parameters to demonstrate therapeutic advantages over conventional formulations.

## 2. MATERIALS AND METHODS

### 2.1 MATERIALS

Danazol (USP grade, 99.5% purity) was obtained from Sciquaint Innovations (Pune, India). Malonic acid, oxalic acid, fumaric acid, and caprylic acid (all analytical grade) were purchased from Sciquaint Chemicals (Pune, India). Microcrystalline cellulose (Avicel PH-102) and sodium croscarmellose (AcDiSol) were procured from FMC Neeta

Chemicals (Pune, India). Polyvinylpyrrolidone K-30, Magnesium stearate and Phosphate buffer pH 6.8 was obtained from Research Lab fine chem industries (Mumbai, India). Danocrine® tablets (200 mg danazol, Sanofi-Aventis, France, Batch No. DAN2023-045, Exp. Date: 12/2025) were procured from licensed pharmacy, (Pune, India). All other chemicals and reagents used were of analytical grade and used as received without further purification.

### 2.2 METHODS

#### 2.2.1 Preparation of Calibration Curve

Calibration curve of danazol was prepared in methanol:phosphate buffer pH 6.8(7:3). Dissolving 100 mg danazol in 100 mL of the solvent mixture prepared a stock solution (1000  $\mu\text{g/mL}$ ). Appropriate dilution of the stock solution was carried out to prepare working standard solutions (5–30  $\mu\text{g/mL}$ ). The absorbance at 286 nm was determined using a UV-visible spectrophotometer (Shimadzu UV-1800, Japan). The absorbance vs concentration calibration curve was drawn and linear regression equation was determined. The values of coefficient of determination ( $R^2$ ), slope and y-intercept were calculated. The limit of detection (LOD) and limit of quantification (LOQ) were determined based on the standard deviation of the response and the slope of the calibration curve using the ICH Q2(R1) guidelines. LOD was calculated as  $3.3 \times \sigma/S$  and LOQ as  $10 \times \sigma/S$ , where  $\sigma$  is the standard deviation of the y-intercept and  $S$  is the slope of the calibration curve [15].

#### 2.2.2 FTIR Analysis

FTIR spectroscopy was employed to assess molecular interactions between danazol and co-formers (malonic acid, oxalic acid, fumaric acid, caprylic acid) in physical mixtures prior to co-crystallization. Approximately 2-3 mg of each sample was placed directly onto the diamond crystal and compressed. Spectra were obtained in the range of 4000-400  $\text{cm}^{-1}$  with a resolution of 4  $\text{cm}^{-1}$ , with 24 scans per spectrum. Characteristic peaks were identified and compared across samples to understand structural changes and intermolecular interactions. Regions near functional groups engaged in hydrogen bonding (carbonyl, hydroxyl and amine groups) were given special attention [16].

#### 2.2.3 Differential Scanning Calorimetry (DSC) Analysis

Thermal behavior of pure components and physical mixtures was characterized using differential scanning calorimetry (DSC 214 Polyma, NETZSCH). Samples (3-5 mg) were accurately weighed and sealed in aluminum pans with pierced lids. An empty aluminum pan was used as reference. Samples were heated from 30°C to 300°C at a heating rate of 10°C/min under nitrogen purge (50 mL/min). The onset temperature, peak temperature, and enthalpy of fusion were recorded. Co-crystal formation was confirmed by comparing thermal profiles of co-crystals with those of pure components and physical mixtures, with particular focus on melting point depression, appearance of new thermal events, and disappearance of endotherms associated with pure components [17,18].

## 2.2.4 Formulation of Co-crystals by Solvent Evaporation

Co-crystals of danazol with various co-formers were prepared using the solvent evaporation technique. Danazol was combined with selected co-formers (malonic acid, oxalic acid, fumaric acid, and caprylic acid; analytical grade, Sciquaint Chemicals, India) in 1:1 and 1:2 ratios. Each mixture was dissolved in 10 mL ethanol (99.9%) in a glass beaker at room temperature ( $25 \pm 2^\circ\text{C}$ ) [19]. Solutions were stirred at 100 rpm for 30 minutes and left undisturbed for 24-72 hours until complete solvent evaporation. The resulting crystals were collected, dried in a desiccator for 24 hours, passed through a #60 mesh sieve, and stored in airtight containers. All preparations were performed in triplicate ( $n=3$ ) [18].

## 2.2.5 Solubility Determination of Danazol Co-crystals

Shake flask method was used to determine aqueous solubility. Each sample was added to 50 mg excess, and 10 mL distilled water in glass vials and agitated in orbital shaker (Thermo Scientific MaxQ 4000) at  $37 \pm 0.5^\circ\text{C}$  and 100 rpm for 48 hours. The suspensions were passed through 0.45  $\mu\text{m}$  membrane filters (Millipore, India). Dilutions of the filtrates were accordingly done, and the concentration of danazol was determined at an  $\lambda_{\text{max}}$  of 286 nm, with a nanomolar concentration range on a UV visible spectrophotometer (Shimadzu UV 1800, Japan). Calibration curves ( $R^2 > 0.999$ ) were set using danazol standards (1-50  $\mu\text{g/mL}$ ) made in the same medium. In triplicate ( $n=3$ ), all measurements were performed [20,21].

**Table 1:** Variables in  $3^2$  Factorial Design for Danazol Co-crystal Tablets

Independent Variables			
Variables	Quantity (mg/tablet)		
	Low (-1)	Medium (0)	High (+1)
X <sub>1</sub> : Sodium Croscarmellose	8.0	16.0	24.0
X <sub>2</sub> : PVP K-30	4.0	12.0	20.0
Dependent Variables			Goal
Y <sub>1</sub> : Disintegration Time (seconds)			Minimize
Y <sub>2</sub> : Drug Release at 30 min (%)			Maximize

## 2.2.6 Experimental Design for Tablet Formulation

A  $3^2$  full factorial design was employed with two independent variables: X<sub>1</sub> (sodium croscarmellose concentration, 8-24mg/Tablet) and X<sub>2</sub> (PVP K-30 concentration, 4-20 mg/Tablet), each at three levels (-1, 0, +1). Nine formulations were prepared according to the design matrix generated using Design-Expert® software (version 13.0, Stat-Ease Inc., USA). The dependent variables were Y<sub>1</sub> (disintegration time) and Y<sub>2</sub> (% drug release at 30 minutes). The mathematical relationship was established using the following equation [22,23].

$$Y = b_0 + b_1X_1 + b_2X_2 + b_{12}X_1X_2 + b_{11}X_1^2 + b_{22}X_2^2 \dots \dots \dots (1)$$

ANOVA was performed to validate the model ( $p < 0.05$  considered significant), and response surface plots were generated to visualize effects of variables on responses.

## 2.2.7 Preparation of Danazol Co-crystal Tablets

Co-crystallization product containing danazol (200mg equiv.) was prepared by direct compression into Danazol tablets. The danazol co-crystal formulation was blended with microcrystalline cellulose (diluent), sodium croscarmellose (superdisintegrant), PVP K-30 (binder), and colloidal silicon dioxide (2.0 mg, 0.5% w/w) for 15 minutes using a laboratory blender. Magnesium stearate (2.0 mg, 0.5% w/w) was then added and mixed for additional 3 minutes to ensure uniform distribution without over-mixing. To that end, the powder blends were compressed using a rotary tablet press (Rimek Mini Press-II) at a compression force of 10 to 12 kN using 10 mm standard concave punches. Therefore, it was kept at  $400 \pm 20$  mg for tablet weight [24,25].

## 2.2.8 Pre-compression Evaluation of Danazol Co-crystal Powder Blends

### a. Angle of Repose

The fixed funnel method was used to determine the angle of repose. A glass funnel with its tip at a fixed height ( $h = 2$  cm) above a flat surface covered with a graph paper was mounted with a 10 mm orifice in the funnel. For the next trial, 10 g powder blend was carefully poured through the funnel until the apex of conical pile reached the apex of the conical pile. Triplicate measurement of the radius ( $r$ ) of the powder cone base was taken from different directions, and the average was calculated. Using the following equation, the angle of repose ( $\theta$ ) was calculated.

$$\theta = \tan^{-1}(h/r) \dots \dots \dots (2)$$

where  $\theta$  is the angle of repose,  $h$  is the height of the pile, and  $r$  is the radius of the base of the powder cone.[26]

### b. Bulk Density and Tapped Density

Bulk and tapped densities were determined using a digital tap density apparatus (Electrolab ETD-1020, India). For bulk density, accurately weighed powder blend (10 g) was gently poured into a 50 mL graduated cylinder. The volume occupied by the powder ( $V_0$ ) was recorded without disturbing the cylinder. The bulk density ( $\rho_b$ ) was calculated using the following equation:

$$\rho_b = m/V_0 \dots \dots \dots (3)$$

where  $\rho_b$  is the bulk density (g/mL),  $m$  is the mass of the powder (g), and  $V_0$  is the unsettled apparent volume (mL).

For tapped density, the same cylinder was mechanically tapped for 500 taps using the tap density apparatus. The final volume ( $V_t$ ) after tapping was recorded, and the tapped density ( $\rho_t$ ) was calculated using the following equation:

$$\rho_t = m/V_t \dots \dots \dots (4)$$

where  $\rho_t$  is the tapped density (g/mL),  $m$  is the mass of the powder (g), and  $V_t$  is the final tapped volume (mL) [27].

**Table 2:** Formulation Composition of Danazol Co-crystal Tablets (mg/tablet)

Ingredients (mg/tablet)	VF1	VF2	VF3	VF4	VF5	VF6	VF7	VF8	VF9
Danazol:Malonic Acid Co-crystal (1:2)	323	323	323	323	323	323	323	323	323
Sodium Croscarmellose	8.0	8.0	8.0	16.0	16.0	16.0	24.0	24.0	24.0
PVP K-30	4.0	12	20	4	12	20	4	12	20
Microcrystalline Cellulose	60.67	52.67	44.67	52.67	44.67	36.67	44.67	36.67	28.67
Colloidal Silicon Dioxide	2.0	2.0	2.0	2.0	2.0	2.0	2.0	2.0	2.0
Magnesium Stearate	2.0	2.0	2.0	2.0	2.0	2.0	2.0	2.0	2.0
Total Weight (mg)	400	400	400	400	400	400	400	400	400

Danazol:Malonic Acid Co-crystal (1:2) contains equivalent of 200 mg Danazol.

### c. Carr's Index and Hausner's Ratio

Carr's index and Hausner's ratio were calculated from the bulk and tapped density values to assess powder flowability and compressibility. Carr's index (CI) was calculated using the following equation:

$$CI = [(\rho_t - \rho_b)/\rho_t] \times 100 \dots \dots \dots (4)$$

where CI is the Carr's index (%),  $\rho_t$  is the tapped density (g/mL), and  $\rho_b$  is the bulk density (g/mL).

Hausner's ratio (HR) was calculated using the following equation:

$$HR = \rho_t/\rho_b \dots \dots \dots (5)$$

where HR is the Hausner's ratio,  $\rho_t$  is the tapped density (g/mL), and  $\rho_b$  is the bulk density (g/mL) [28].

### 2.2.9 Post-compression Evaluation of Danazol Co-crystal Tablets

#### a. General Appearance and Organoleptic Properties

Shape, color uniformity, presence of cracks, chips and surface texture of the compressed tablets were visually examined. The experiment was performed under standard lighting in a white background. The tablets were also judged by a panel of 3 trained evaluators regarding their odour and taste properties. These sensory assessments were described based on established terminologies from USP guidelines [29].

#### b. Weight Variation

The USP <905> specifications for weight variation test were performed. Every batch of 20 tablets were randomly selected and weighed individually by an analytical balance (Mettler Toledo, Switzerland) with a precision of 0.1 mg. The weight and standard deviation were both calculated. The test conforms to USP specifications for tablet weights greater than 324 mg on not more than 2 of the individual weights deviating from the average weight by more than 5% and not more than 10% Using the following equation, the weight variation was calculated:[30]

$$\text{Weight variation} = ((\text{Individual wt.} - \text{Average wt.})/(\text{Average weight})) \times 100 \dots \dots \dots (6)$$

### c. Thickness

The thickness of 10 temperature controlled tablets of each batch was measured with a digital vernier caliper (Mitutoyo, Japan) with a precision of 0.01 mm. Thickness of each tablet was recorded by placing it in between the jaws of the caliper. Calculations were made for the mean thickness and its standard deviation. The variation in the thickness accepted at  $\pm 5\%$  of average value. Each tablet was measured in triplicate (n=3) for each [31].

### d. Hardness

Using a digital tablet hardness tester (Electrolab EH-01) hardness of tablets was determined. In fact, each batch was randomly selected ten tablets, and their weights were compared with that of our reference weights. The hardness tester has a clamp and some tablets were placed between the jaws of the clamp in the same orientation and force was applied until the tablet fractured. The kilograms of force recorded was only kgf. The mean hardness and standard deviation were obtained. A hardness range of 5-7 kgf was aimed at as per the target hardness range appropriate for immediate release tablets. Replications were made on triplicate (n=3) [32].

### e. Friability

Friability test was conducted according to USP <1216> specifications using a Roche friabilator (Electrolab EF-2, India). Twenty tablets were randomly selected, de-dusted, and accurately weighed ( $W_1$ ). The tablets were placed in the friabilator drum and subjected to 100 rotations in 4 minutes (25 rpm). After the test, the tablets were carefully de-dusted and reweighed ( $W_2$ ). The percentage friability was calculated using the following equation:[33]

$$\text{Friability (\%)} = [(W_1 - W_2)/W_1] \times 100 \dots \dots \dots (7)$$

where  $W_1$  is the initial weight of tablets and  $W_2$  is the weight of tablets after the test. As per USP specifications, the friability value should be less than 1% for conventional tablets. All measurements were performed in triplicate (n=3).

### f. Disintegration Time

A disintegration test apparatus (Electrolab ED-2L India) was used for a disintegration test according to USP <701> and disintegration time was evaluated. For each batch, six tablets were placed in the six tubes of the basket rack assembly individually. The immersion fluid of phosphate

buffer pH 6.8 at  $37 \pm 0.5^\circ\text{C}$  was placed in a 1 liter beaker and the assembly was positioned within that. A frequency of 29-32 cycles per minute was applied to the basket rack, and the basket rack was moved vertically a distance of 53-57 mm. The time elapse was recorded for when the tablet was completely disintegrated leaving no palpable mass within the tube. The disintegration time of the immediate release tablet should be less than 30 minutes as per USP specifications. Measurements were taken three times ( $n=3$ ) [34].

#### g. Drug Content Uniformity

According to USP <905>, the uniformity of the drug content was established. Each batch of ten tablets were subjected to random selection of tablets and individual assay. They were crushed with a mortar and pestle and transferred to a 100 mL volumetric flask. The drug was sonicated in 70 mL of methanol:phosphate buffer pH 6.8 (7:3) to ensure complete extraction of the drug about 15 minutes. The same solvent was added to the volume to 100 mL, and then the solution was filtered through a  $0.45\ \mu\text{m}$  membrane filter. The filtrate was then appropriately diluted and there was a measurement of the absorbance at 286 nm using a UV-visible spectrophotometer (Shimadzu UV-1800, Japan) [35].

#### h. In-vitro Dissolution Studies

These were then performed in-vitro by the USP Type II (paddle) apparatus (Electrolab TDT-08L, India) with USP <711> specifications. The dissolution medium was a 900 mL phosphate buffer pH 6.8, which was maintained at  $37 \pm 0.5^\circ\text{C}$ . Phosphate buffer pH 6.8 was selected as it represents the physiological pH of the small intestine where danazol absorption occurs, and is recommended by USP <711> for BCS Class II drugs to provide biorelevant dissolution conditions. The speed of rotation of the paddle was 75 rpm. Six dissolution vessels were used and each one had one tablet in it. The measure of sink conditions was achieved by withdrawn of samples (5 mL) at predetermined time intervals (5, 10, 15, 30, 45, and 60 minutes) and replaced with an equal volume of fresh dissolution medium. Drug content in the samples was measured by filtering them through a  $0.45\ \mu\text{m}$  membrane filter and analyzing them using UV-visible spectrophotometer (Shimadzu UV-1800, Japan) at 286 nm. All the measurements performed in triplicate ( $n=3$ ) [36].

#### i. Accelerated Stability Study

Guidelines according to ICH Q1A(R2) were followed for accelerated stability studies. It was formulated optimised, packed in aluminum blister packs, and stored in stability chambers (Thermo Scientific) under accelerated conditions ( $40 \pm 2^\circ\text{C}/75 \pm 5\% \text{ RH}$ ) for three months. Predefined time points (0, 1, 2 and 3 months) samples were withdrawn and physical appearance, hardness, disintegration time, drug content and in-vitro dissolution were evaluated [37].

### 3. Results

#### 3.1 Calibration curve of Danazol

The calibration curve of Danazol exhibited excellent linearity ( $R^2 = 0.9985$ ) with the equation  $y = 0.0075x - 0.0018$ , confirming the reliability of the analytical method (Figure 2). The strong linear relationship between concentration and absorbance, coupled with the minimal y-intercept, indicates negligible systematic error, establishing

a robust foundation for quantitative determination of Danazol in the co-crystal formulations. Method validation was performed according to ICH Q2(R1) guidelines. Precision ( $\text{RSD} < 2\%$ ), accuracy (98-102% recovery), and linearity ( $R^2 > 0.9985$ ) were confirmed within the concentration range. The calculated LOD and LOQ values were  $0.24\ \mu\text{g/mL}$  and  $0.73\ \mu\text{g/mL}$ , respectively, confirming the method's sensitivity for danazol quantification within the studied concentration range

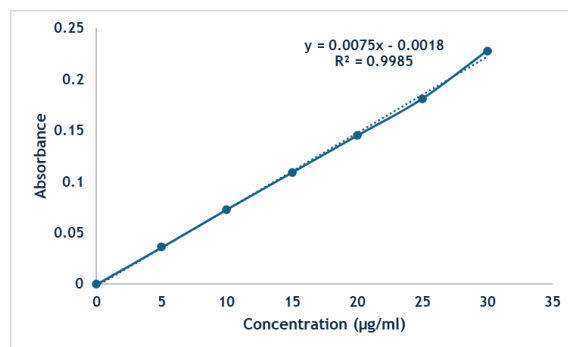


**Fig 2:** Calibration curve of danazol in methanol:phosphate buffer pH 6.8 (7:3). Linear relationship showing  $R^2 = 0.9985$  with equation  $y = 0.0075x - 0.0018$  ( $n=3$ ).

#### 3.2 Results of FTIR analysis

Fourier Transform Infrared (FTIR) spectroscopy was employed to evaluate potential drug-excipient interactions in the physical mixture. The FTIR spectrum of pure Danazol (Figure 3A) exhibited characteristic peaks at 3895.11, 3824.51, and  $3732.04\ \text{cm}^{-1}$  corresponding to O-H stretching vibrations, while the aliphatic C-H stretching was observed at  $2975.56\ \text{cm}^{-1}$ . The ketone C=O stretching appeared at  $1695.73\ \text{cm}^{-1}$ , and aromatic C=C stretching was detected at  $1571.62\ \text{cm}^{-1}$ . The physical mixture (Figure 3B) retained most of the characteristic peaks of Danazol with minor shifts, showing O-H stretching at 3879.59, 3788.56, 3741.29, and  $3635.29\ \text{cm}^{-1}$ , and aliphatic C-H stretching at  $3024.60\ \text{cm}^{-1}$ . A new peak at  $2106.96\ \text{cm}^{-1}$  was observed in the physical mixture. This peak likely represents a combination band or overtone arising from C-H stretching vibrations, indicating molecular interactions between danazol and co-formers without covalent bond formation. The persistence of characteristic peaks of Danazol in the physical mixture with only slight shifts in wavenumbers indicates the absence of significant chemical interactions between the drug and excipients, confirming compatibility for the co-crystal formulation.

#### 3.3 Differential Scanning Calorimetry

The thermal behavior of Danazol and its physical mixture with excipients was investigated using Differential Scanning Calorimetry (DSC), as depicted in Figure 4. Pure Danazol (Figure 4A) exhibited a sharp endothermic peak at  $226.33^\circ\text{C}$ , corresponding to its melting point and indicating the crystalline nature of the drug. The DSC thermogram of the physical mixture (Figure 4B) revealed two distinct endothermic peaks: one at  $186.63^\circ\text{C}$ , likely attributable to the melting of one of the excipients, and a second peak at  $226.63^\circ\text{C}$ , which corresponds closely to the melting point of pure Danazol. The preservation of Danazol's characteristic melting peak in the physical mixture, with only a negligible shift from  $226.33^\circ\text{C}$  to  $226.63^\circ\text{C}$  ( $\Delta T = 0.3^\circ\text{C}$ ), suggests no interaction between the drug and excipients during the thermal process.

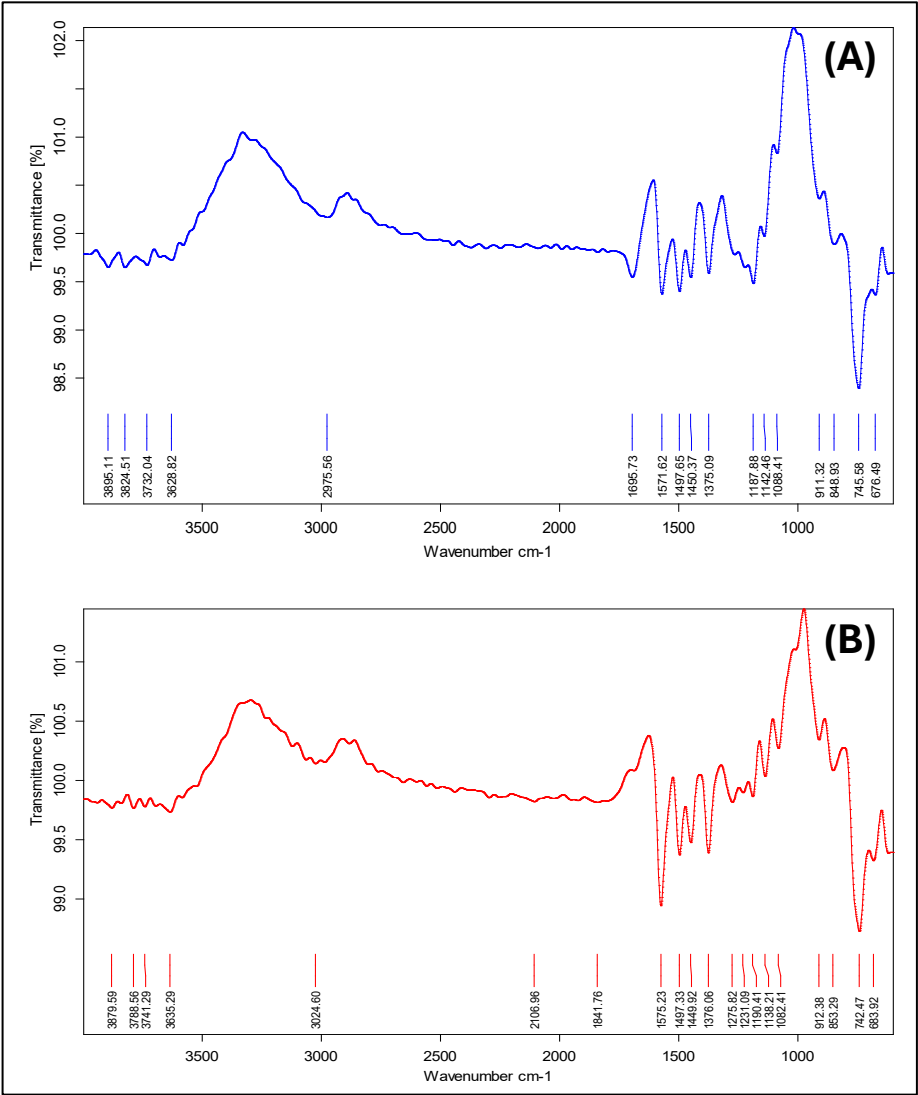


Fig. 3: FTIR Spectral analysis of (A) Danazol and (B) physical mixture (Drug + Excipient)

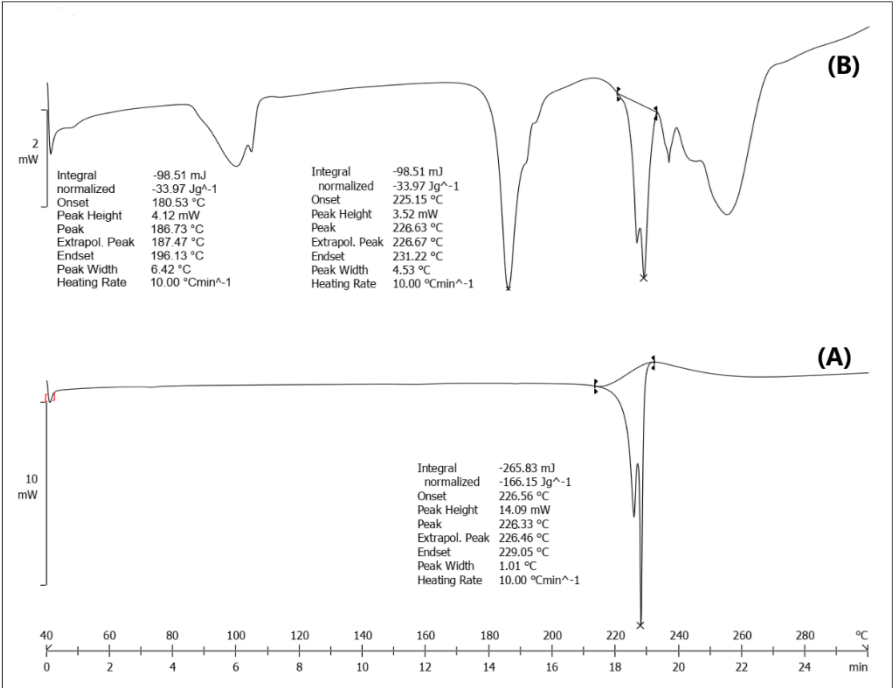


Fig. 4: DSC Thermogram of (A) Danazol (226.33 °C) and (B) physical mixture (Drug + Excipient) (186.63, 226.63 °C)

### 3.4 Characterization of Danazol Co-crystals

The aqueous solubility of Danazol was significantly enhanced through co-crystallization with various co-formers, as demonstrated in Table 3. Among all co-crystals tested, Danazol: Malonic acid in a 1:2 ratio exhibited the highest solubility enhancement ( $11.42 \pm 0.53 \mu\text{g/mL}$ ), representing a remarkable 13.76-fold increase compared to pure Danazol ( $0.83 \pm 0.12 \mu\text{g/mL}$ ). A clear trend was observed wherein 1:2 ratios consistently outperformed their 1:1 counterpart for all co-formers, with the effectiveness following the order: malonic acid > fumaric acid > oxalic acid > caprylic acid. This substantial improvement in aqueous solubility through co-crystallization techniques suggests potential for enhanced bioavailability of Danazol in the final formulation.

**Table 3:** Comparative Aqueous Solubility Enhancement of Danazol Co-crystals with Various Co-formers at 37°C (n=3)

Formulation	Drug: Co-former Ratio	Aqueous Solubility ( $\mu\text{g/mL}$ )	Fold Increase in Solubility
Pure Danazol	-	$0.83 \pm 0.12$	1.00
Danazol: Malonic acid	1:1	$5.75 \pm 0.41$	6.93
Danazol: Oxalic acid	1:1	$3.82 \pm 0.32$	4.60
Danazol: Fumaric acid	1:1	$4.67 \pm 0.29$	5.63
Danazol: Caprylic acid	1:1	$2.16 \pm 0.22$	2.60
Danazol: Malonic acid	1:2	$11.42 \pm 0.53$	13.76
Danazol: Oxalic acid	1:2	$6.21 \pm 0.38$	7.48
Danazol: Fumaric acid	1:2	$7.35 \pm 0.44$	8.86
Danazol: Caprylic acid	1:2	$3.19 \pm 0.31$	3.84

Values represent mean  $\pm$  standard deviation (n=3)

### 3.5 X-ray diffraction study

The X-ray diffraction (XRD) spectrum of Danazol:Malonic acid co-crystals (D-MA-CO) presented in Figure 5 reveals distinct crystalline characteristics with sharp, high-intensity diffraction peaks primarily concentrated between  $15^\circ$  and  $25^\circ$   $2\theta$  values. The prominent peaks observed at approximately  $19^\circ$  and  $21^\circ$   $2\theta$  with intensity values exceeding 2000 and 3000 counts, respectively, indicate a well-defined crystalline structure with high degree of structural order. XRD analysis confirmed distinct crystalline phases different from pure components, ruling out hydrotropic solubilization. The 1:2 stoichiometric advantage reflects co-crystal thermodynamic stability rather than concentration-dependent hydrotropic effects.

### 3.6 Pre-compression Evaluation Parameters Danazol Co-crystals Tablet

The pre-compression evaluation of Danazol co-crystal powder blends, detailed in Table 4, revealed favorable flow characteristics across most formulations. Formulations VF3 and VF7 demonstrated excellent flow properties, with the lowest angles of repose ( $27.5 \pm 0.7^\circ$  and  $26.8 \pm 0.7^\circ$ , respectively) and Hausner's ratios ( $1.12 \pm 0.01$  and  $1.08 \pm 0.01$ , respectively). Notably, VF7 exhibited superior compressibility with the lowest Carr's index ( $7.4 \pm 0.5\%$ ), indicating optimal packing properties. The bulk densities

ranged from  $0.368 \pm 0.014$  to  $0.412 \pm 0.011 \text{ g/mL}$ , while tapped densities varied between  $0.432 \pm 0.011$  and  $0.462 \pm 0.012 \text{ g/mL}$  across all formulations. Formulations VF4 and VF8 displayed relatively poorer flow characteristics with higher angles of repose ( $32.6 \pm 0.9^\circ$  and  $33.1 \pm 0.9^\circ$ , respectively) and Carr's indices ( $16.6 \pm 0.8\%$  and  $16.0 \pm 0.8\%$ , respectively), categorized as "Fair." Overall, most of the powder blends exhibited good to excellent flow properties, suggesting their suitability for direct compression tablet manufacturing.

### 3.7 Post-compression Evaluation Parameters Danazol Co-crystals Tablet

To evaluate the physical and the chemical properties of the co-crystal tablets of Danazol, the following post-compression analysis was done. The data presented in Table 5 demonstrate that all formulations (VF1-VF9) exhibited similar organoleptic characteristics, characterized by off-white, round, flat-faced table with smooth surface, no odor activity, and slightly bitter taste sensation. From the physical parameters presented in the Table 6 it was observed that the tablet profile of all formulations was uniform and their average Wt. was in between  $398.9 \pm 4.7 \text{ mg}$  to  $401.3 \pm 3.1 \text{ mg}$  which was within limit of pharmacopoeial standards. The thickness of the tablets has not changed significantly with an average of  $3.74 \pm 0.03$  -  $3.83 \pm 0.08 \text{ mm}$  whereas the hardness of the tablets was different varying from  $39.7 \pm 3.7 \text{ N}$  for VF7 to  $68.9 \pm 3.4 \text{ N}$  for VF3 evidencing the difference in the compression profiles. Table 7 also showed that formulation VF7 disintegrated within the shortest time of  $63 \pm 8$  seconds, however it had slightly low drug content of  $96.9 \pm 1.7\%$  and high friability of  $0.86\%$ . VF3, however, disintegrated in a longer duration of  $312 \pm 22$  seconds, but the drug content uniformity high at  $101.3 \pm 1.2\%$  and friability low at only  $0.32\%$ . Concerning the drug content, all formulations were within the acceptable range of  $96.9$  to  $101.3\%$  and friability less than  $1\%$  thus conforming to the pharmacopoeial requirement. However, a correlation between hardness, disintegration time, and friability was observed across the various formulation.

### 3.7 Optimization of Results for Danazol Co-crystal Tablets

#### 3.7.1 Disintegration Time ( $Y_1$ )

As shown in the Table 8, for the disintegration time, the employed quadratic model had the acceptance level of 0.0181, an overall performance assessed by rather high values of adjusted  $R^2$  (0.9971) and predicted  $R^2$  (0.9890). The small difference in these  $R^2$  values (0.0081) suggested that the model had a high test accuracy, so the model was not over-fitted to the experimental data. The residual analysis including the ANOVA results of the quadratic model (Table 9) is as follows; The F-value value of the model is 547.22 and the p value is 0.0001 which indicates the less than 0.01% chances that such a big F value originated from noise. These independent variables showed significant impact on disintegration time, however out of both Na CCP (factor A) has significant impact to the highest extent as F-value is 1853.07 and the p-value  $<0.0001$ , followed by PVP K-30 (factor B) in which  $F=810.45$  and  $p<0.0001$ . These include interaction term AB, quadratic terms  $A^2$  and  $B^2$  which were also significant with F-value of 32.15 ( $p=0.0109$ ), 29.19 ( $p=0.0124$ ) and 11.26 ( $p=0.0439$ ) respectively, thus validating the use of quadratic model.

The polynomial equation derived for disintegration time was:

$$Y_1 = 154.78 - 72.83A + 48.17B - 11.75AB + 15.83A^2 + 9.83B^2 \dots\dots\dots(9)$$

The disintegration time results in terms of contour and response surface plots of A and B factors are depicted in the Figure 6A and 5B respectively. This shows that as the amount of sodium croscarmellose increased, the disintegration time reduced as portrayed by the negative coefficient of A of -72.83 while as the amount of PVP K-30 increased, the disintegration time increased as reflected by the positive coefficient of B of +48.17. Figure 6A shows the curved straight line which indicated the quadratic relationship while figure 6B shows the twisted hyperbolic surface showing the interaction of the two variables. The disintegration time variation was from 74 seconds (high sodium croscarmellose, low PVP K-30) to 312 seconds (low sodium croscarmellose, high PVP K-30) thus proving the impact of varying concentrations of the excipients on this parameter. The results obtained from the plots also indicated that the sodium croscarmellose, highest in concentration at 24 mg showed the minimum disintegration time while the minimum concentration of PVP K-30 of 4 mg was sufficient.

### 3.7.2 Drug Release at 30 minutes ( $Y_2$ )

Regarding model selection for drug release at 30 minutes as shown in Table 8, it was found that the quadratic model was the most suitable for the model as it has a significant F-value of ( $p=0.0104$ ) with reasonable adjusted  $R^2$  (0.9483) and predicted  $R^2$  (0.7994). The results of ANOVA analysis of quadratic model (Table 9) where the F value is 30.33 and p value is 0.0090 show the chances are only 0.90% for such large F value due to noise. The ANOVA results indicated that, sodium croscarmellose concentration (Factor A) was found to have a significant effect on drug release (F-value=67.82,  $p=0.0037$ ) and ranked high compared to PVP K-30 concentration (Factor B, F-value=23.65,  $p=0.0166$ ). The results showed that  $A^2$  was significant at F-value 59.22 and  $p=0.0046$  while the AB and  $B^2$  were statistically insignificant at  $p>0.05$  which depicts that the effect of sodium croscarmellose is not simple on drug release pattern while on the other hand the use PVP K-30 seem to have a very little complex relationship as it showed the relation of a straight line.

The polynomial equation established for drug release at 30 minutes was:

$$Y_2 = 79.67 + 9.48A - 5.60B - 0.8750AB - 15.35A^2 + 1.50B^2 \dots\dots\dots(10)$$

The contour and response surface plots in Figure 6C and 5D showed the quadratic relationship of the variables and drug release at 30 minutes. The positive linear coefficient of A(+9.48) showed that with increasing sodium croscarmellose concentration, the drug release was initially increasing, however there was a more important negative quadratic component of sodium croscarmellose concentration ( $-15.35A^2$ ) where the drug release started to decrease at higher concentration levels. This was in line with the results obtained from the fairly curved elliptical contour lines in figure 5C and the sharp curvature of the response surface in Figure 6D. The negative coefficient of B (-5.60) was in line with the decreasing drug release that was observed when the concentration of PVP K-30 was increased. The results in figure 4 also revealed that the highest amount of drug

release is 83.6% at moderate to high sodium croscarmellose (16 to 24 mg) with low edetate PVP K30 (4 mg) while the lowest one is 50.8% at low sodium croscarmellose (8 mg) and high PVP K-30 (20 mg). The plots showed an area of highest drug release rates rather than a precise rate, and both the formulations containing 16 to 24 mg of sodium croscarmellose and 4 mg of PVP K-30 showed comparable dissolution profile.

### 3.8 Validation of optimization

Based on the factorial design optimization, formulation VF7 with 24 mg sodium croscarmellose and 4 mg PVP K-30 was identified as the optimized formulation with maximum desirability (1.000), as shown in Table 10. The optimization was performed with the goals of minimizing disintegration time and maximizing drug release at 30 minutes. The experimental values of the optimized formulation (VF7) were in excellent agreement with the predicted values, with percent error of 0.26% for disintegration time and 0.00% for drug release at 30 minutes. This remarkable correlation between predicted and experimental values confirms the high reliability and predictive capability of the developed quadratic models for both responses. The optimized formulation demonstrated superior performance with rapid disintegration (74 seconds) and enhanced drug release (83.6% at 30 minutes), making it an ideal candidate for further development of Danazol co-crystal tablets with improved dissolution characteristics.

### 3.9 In-vitro Dissolution Profiles

Details of in vitro dissolution studies of danazol co-crystal tablets are presented in figure 7, where it was observed that all the nine formulations showed considerable difference in the release profile. Formulation VF7 proved to have the highest dissolution profile with greater cumulative release of the drug at all time intervals and at 5 min, the release was of  $30.5 \pm 2.2\%$  and at 60min the release achieved was  $95.8 \pm 2.0\%$ . The dissolution rates of formulations VF4 and VF5 were improved as  $93.8 \pm 2.0$  and  $94.2 \pm 1.9\%$  at 60 min. On the other hand, formulations VF1-VF3 had distinctly slower release profiles, with the VF3 possessing the least amount of cumulative release ( $70.6 \pm 2.2\%$ ) in 60 min, which also had the highest hardness and the slowest disintegration time. The dissolution profiles of developed VF7 formulation as compared with the marketed product Danocrine® are compared in Figure 8 for comparative dissolution study, in which VF7 formulation releases approximately more than two folds amount of the drug at the initial time of 5minute ( $30.5 \pm 2.2\%$  of VF7 vs  $14.2 \pm 1.8\%$  of Danocrine®) and more than 95% of VF7 formulation up to 60 minutes while only  $75.2 \pm 2.7\%$  of marketed Danocrine formulation during the same period. Statistical comparison using similarity factor ( $f_2$ ) methodology showed  $f_2 < 50$  between VF7 and Danocrine®, confirming statistically significant differences in dissolution profiles ( $p < 0.05$ , unpaired t-test). The dissolution efficiency (DE30min) for VF7 was  $78.2 \pm 2.1\%$  compared to  $45.3 \pm 1.8\%$  for Danocrine® ( $p < 0.001$ ).



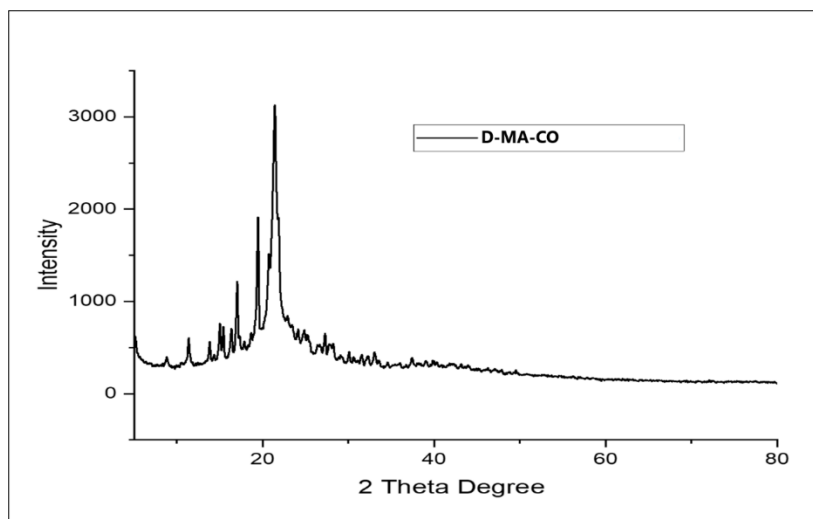


Fig. 5: XRD Spectrum of Danazol: Malonic acid co-crystals

Table 4: Pre-compression Evaluation Parameters of Danazol Co-crystal Powder Blends (n=3)

F. Code	Angle of Repose (°)*	Bulk Density (g/mL)*	Tapped Density (g/mL)*	Carr's Index (%)*	Hausner's Ratio*	Flow Character
VF1	30.2 ± 0.8	0.372 ± 0.013	0.432 ± 0.011	13.9 ± 0.7	1.16 ± 0.01	Good
VF2	28.7 ± 0.6	0.395 ± 0.015	0.449 ± 0.012	12.0 ± 0.5	1.14 ± 0.01	Good
VF3	27.5 ± 0.7	0.410 ± 0.012	0.458 ± 0.014	10.5 ± 0.6	1.12 ± 0.01	Excellent
VF4	32.6 ± 0.9	0.368 ± 0.014	0.441 ± 0.013	16.6 ± 0.8	1.20 ± 0.02	Fair
VF5	30.9 ± 0.7	0.386 ± 0.011	0.451 ± 0.015	14.4 ± 0.7	1.17 ± 0.01	Good
VF6	29.3 ± 0.8	0.404 ± 0.013	0.462 ± 0.012	12.6 ± 0.6	1.14 ± 0.01	Good
VF7	26.8 ± 0.7	0.412 ± 0.011	0.445 ± 0.012	7.4 ± 0.5	1.08 ± 0.01	Excellent
VF8	33.1 ± 0.9	0.374 ± 0.012	0.445 ± 0.013	16.0 ± 0.8	1.19 ± 0.02	Fair
VF9	31.8 ± 0.8	0.392 ± 0.014	0.453 ± 0.015	13.5 ± 0.7	1.16 ± 0.01	Good

\*Values represent mean ± standard deviation (n=3)

Table 5: General Appearance and Organoleptic Properties of Danazol Co-crystal Tablets

F. Code	Color	Shape	Surface Texture	Odor	Taste
VF1	Off-white	Round, flat-faced	Smooth	Odorless	Slightly bitter
VF2	Off-white	Round, flat-faced	Smooth	Odorless	Slightly bitter
VF3	Off-white	Round, flat-faced	Smooth	Odorless	Slightly bitter
VF4	Off-white	Round, flat-faced	Smooth	Odorless	Slightly bitter
VF5	Off-white	Round, flat-faced	Smooth	Odorless	Slightly bitter
VF6	Off-white	Round, flat-faced	Smooth	Odorless	Slightly bitter
VF7	Off-white	Round, flat-faced	Smooth	Odorless	Slightly bitter
VF8	Off-white	Round, flat-faced	Smooth	Odorless	Slightly bitter
VF9	Off-white	Round, flat-faced	Smooth	Odorless	Slightly bitter

Table 6: Physical Parameters of Danazol Co-crystal Tablets

Formulation	Weight Variation* (mg)	Thickness* (mm)	Hardness* (N)
VF1	401.2 ± 4.3	3.82 ± 0.06	48.3 ± 3.2
VF2	399.7 ± 3.8	3.78 ± 0.05	57.6 ± 2.9
VF3	400.5 ± 3.2	3.75 ± 0.04	68.9 ± 3.4
VF4	398.9 ± 4.7	3.81 ± 0.07	44.1 ± 3.5
VF5	400.8 ± 3.5	3.77 ± 0.05	54.8 ± 2.8
VF6	401.3 ± 3.1	3.74 ± 0.03	65.2 ± 3.1
VF7	399.2 ± 5.1	3.83 ± 0.08	39.7 ± 3.7
VF8	400.6 ± 4.2	3.79 ± 0.06	49.5 ± 3.3
VF9	399.8 ± 3.6	3.76 ± 0.04	61.1 ± 2.7

\*Values represent mean ± standard deviation, n=20 for Weight Variation; n=10 for Thickness and Hardness

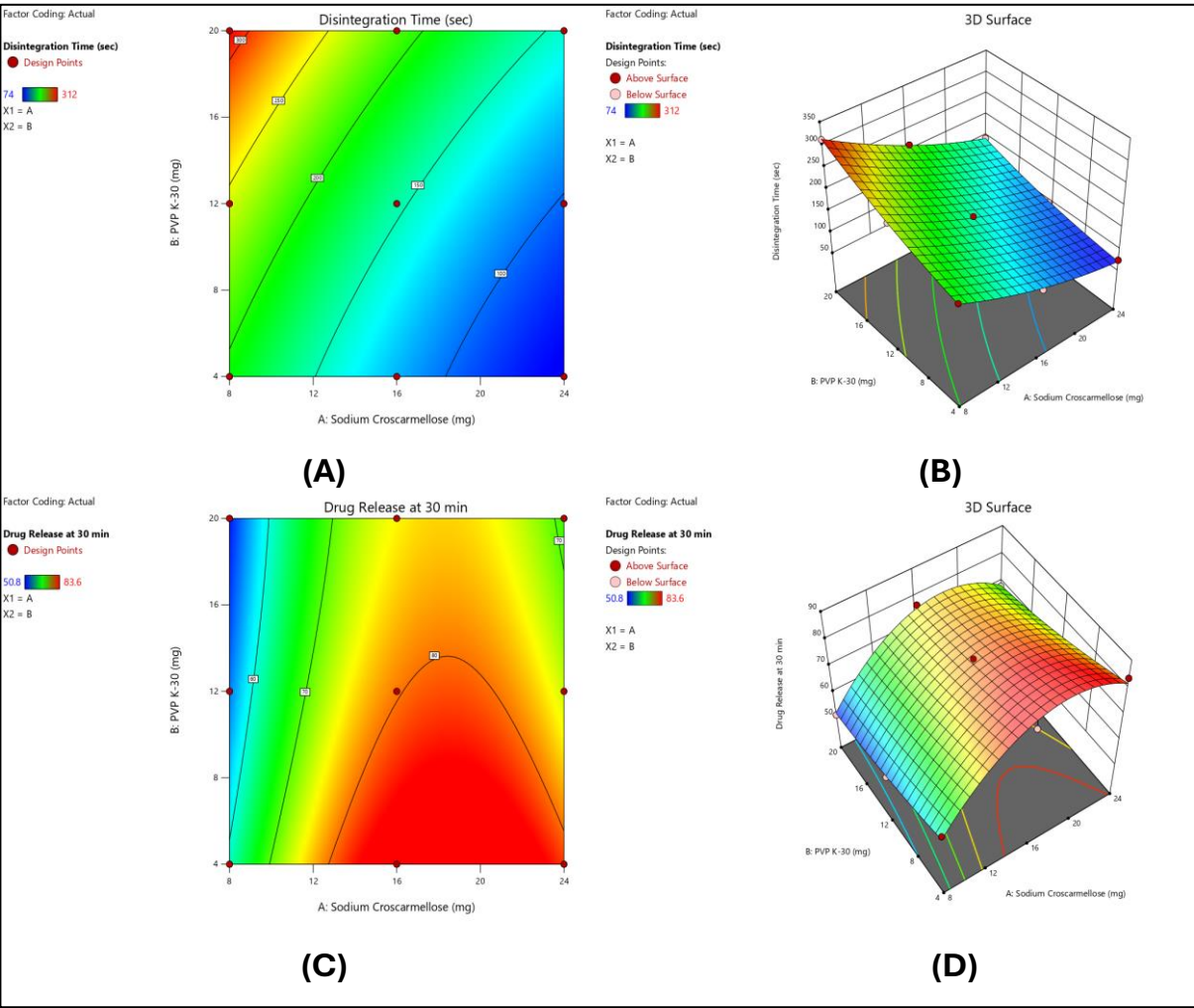
Table 7: Disintegration Time, Drug Content, and Friability of Danazol Co-crystal Tablets

Formulation	Disintegration Time* (seconds)	Drug Content* (%)	Friability (%)
VF1	195 ± 14	98.2 ± 1.5	0.63
VF2	243 ± 17	99.1 ± 1.3	0.48
VF3	312 ± 22	101.3 ± 1.2	0.32
VF4	112 ± 10	97.8 ± 1.6	0.75
VF5	158 ± 13	98.7 ± 1.4	0.54
VF6	214 ± 16	99.5 ± 1.1	0.41
VF7	63 ± 8	96.9 ± 1.7	0.86
VF8	95 ± 11	97.6 ± 1.5	0.67
VF9	144 ± 14	98.9 ± 1.3	0.49

\*Values represent mean ± standard deviation, n=6 for Disintegration Time; n=10 for Drug Content; n=20 for Friability

Table 8: Model Selection Summary for Disintegration Time and Drug Release Responses					
Response	Source	Sequential p-value	Adjusted R <sup>2</sup>	Predicted R <sup>2</sup>	Suggested Model
Disintegration Time (Y1)	Linear	< 0.0001	0.9632	0.9241	
	2FI	0.1124	0.9746	0.9050	
	Quadratic	0.0181	0.9971	0.9890	Suggested
	Cubic	0.6733	0.9960	0.9095	Aliased
Drug Release at 30 min (Y2)	Linear	0.0682	0.4553	0.2029	
	2FI	0.8679	0.3503	-0.2284	
	Quadratic	0.0104	0.9483	0.7994	Suggested
	Cubic	0.6243	0.9395	-0.3779	Aliased

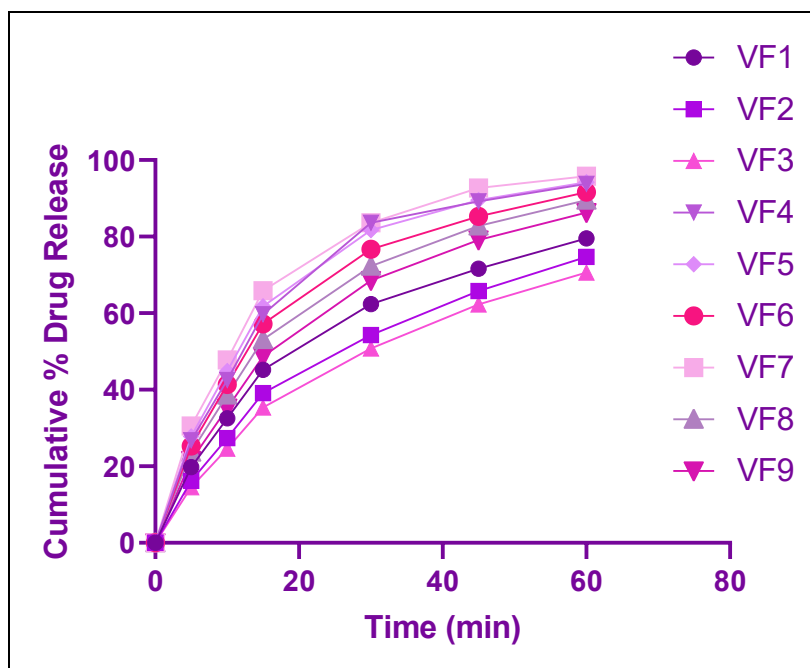
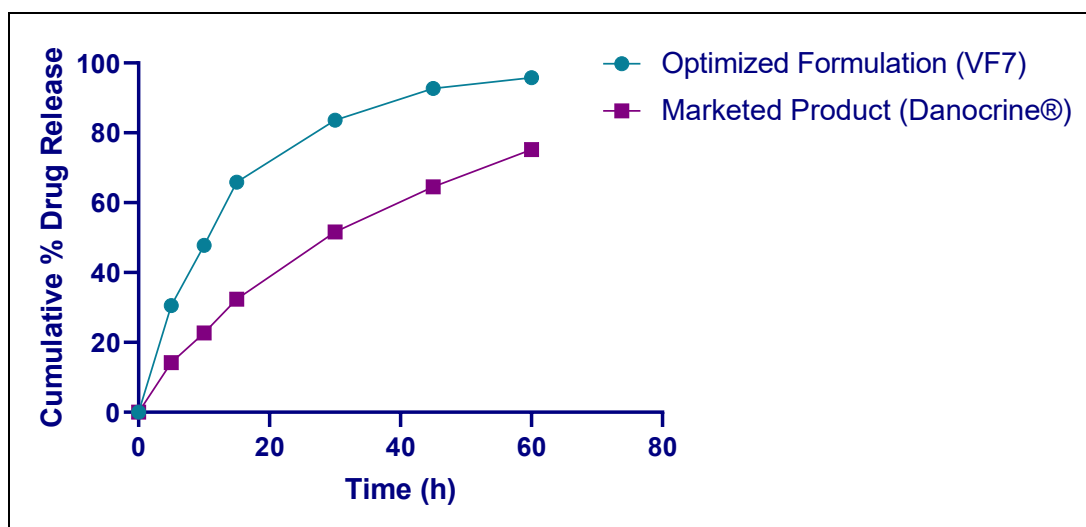
Table 9: ANOVA Results for Disintegration Time and Drug Release at 30 min (Quadratic Models)							
Response	Source	Sum of Squares	df	Mean Square	F-value	p-value	Significance
Disintegration Time (Y1)	Model	46995.36	5	9399.07	547.22	0.0001	Significant
	A-Sodium Croscarmellose	31828.17	1	31828.17	1853.07	< 0.0001	
	B-PVP K-30	13920.17	1	13920.17	810.45	< 0.0001	
	AB	552.25	1	552.25	32.15	0.0109	
	A <sup>2</sup>	501.39	1	501.39	29.19	0.0124	
	B <sup>2</sup>	193.39	1	193.39	11.26	0.0439	
Drug Release at 30 min (Y2)	Model	1206.57	5	241.31	30.33	0.0090	Significant
	A-Sodium Croscarmellose	539.60	1	539.60	67.82	0.0037	
	B-PVP K-30	188.16	1	188.16	23.65	0.0166	
	AB	3.06	1	3.06	0.3849	0.5789	
	A <sup>2</sup>	471.25	1	471.25	59.22	0.0046	
	B <sup>2</sup>	4.50	1	4.50	0.5655	0.5067	



**Fig. 6:** Impact of excipient concentrations on critical quality attributes of Danazol co-crystal tablets. (A) Contour plot and (B) Response surface plot showing effect of sodium croscarmellose and PVP K-30 concentrations on disintegration time; (C) Contour plot and (D) Response surface plot illustrating the influence of the same variables on drug release at 30 minutes.

**Table 10:** Comparison of Predicted and Experimental Results for the Optimized Danazol Co-crystal Tablet Formulation

Formulation	Composition	Predicted Values	Experimental Values	Percent Error (%)
Optimized Formulation	Sodium Croscarmellose (mg)	24.00	24.00	0.00
	PVP K-30 (mg)	4.00	4.00	0.00
	Disintegration Time (seconds)	74.19	74.00	0.26
	Drug Release at 30 min (%)	83.60	83.60	0.00
	Desirability	1.000	-	-

**Fig. 7:** In-vitro Dissolution Profiles of Danazol Co-crystal Tablets in Phosphate Buffer pH 6.8**Fig. 8:** Comparative dissolution profiles of optimized danazol co-crystal tablet formulation (VF7) and marketed product (Danocrine®) in phosphate buffer pH 6.8. Data represent mean  $\pm$  SD (n=6).**Table 14:** Accelerated Stability study data for optimized Danazol co-crystal tablet Formulation (VF7) at  $40 \pm 2^\circ\text{C}/75 \pm 5\% \text{RH}$ 

Parameter	Initial (0 month)	1 month	2 months	3 months
Physical Appearance	Off-white, round, flat tablets with smooth surface	No change	No change	No change
Average Weight (mg)	$400.2 \pm 2.3$	$400.4 \pm 2.6$	$400.5 \pm 2.4$	$400.7 \pm 2.7$
Hardness (N)	$57.8 \pm 2.4$	$58.2 \pm 2.7$	$58.6 \pm 2.5$	$59.3 \pm 2.9$
Disintegration Time (seconds)	$74.0 \pm 3.2$	$75.4 \pm 3.6$	$77.2 \pm 3.8$	$79.5 \pm 4.1$
Drug Content (%)	$99.7 \pm 1.1$	$99.3 \pm 1.3$	$98.9 \pm 1.4$	$98.4 \pm 1.5$
Drug Release at 30 min (%)	$83.6 \pm 3.4$	$82.8 \pm 3.6$	$81.9 \pm 3.7$	$81.2 \pm 3.9$

### 3.10 Accelerated Stability Study

The accelerated stability study of the optimized Danazol co-crystal tablet formulation VF7 was performed at the condition of  $40 \pm 2^\circ\text{C}/75 \pm 5\% \text{ RH}$  for three months and the results of stability are also shown in Table 14. The characteristics of the tablets were kept constant in terms of colour, shape and surface finish as they retained off white color, round shaped and smooth to the touch right from the beginning of the study until the end. The average tablet weight remained close to each other, thus signifying that the physical stability was good at both initial time ( $400.2 \pm 2.3 \text{ mg}$ ) and 3 months ( $400.7 \pm 2.7 \text{ mg}$ ). The hardness of the tablet has the tendency to slightly increase from  $57.8 \pm 2.4 \text{ N}$  in the beginning up to  $59.3 \pm 2.9 \text{ N}$  after 3 months smaller increase in the disintegration time from  $74.0 \pm 3.2 \text{ sec}$  to  $79.5 \pm 4.1 \text{ sec}$  was observed as well. The levels of the drug also remained quite favorable and there was a slight drop of only 0.7% from the initial concentration of  $99.7 \pm 1.1\%$  to the final concentration of  $98.4 \pm 1.5\%$  after the three months. Also, the dissolution profiles were present good profile as at 30 minutes the % drug release slightly reduced to  $81.2 \pm 3.9\%$  from  $83.6 \pm 3.4\%$  at the first instance.

### 4. Discussion

Danazol co-crystals represent a recent advancement for this BCS Class II drug, as poor solubility has been a significant limitation to the compound's effectiveness of the drug especially when used to treat endometriosis. Regarding the calibration study, the linearity resembled a high level of linearity (See figure 2  $R^2 = 0.9985$ ) making it constructive in quantitative measures during this study. The FTIR and DSC results for the sample further supported the claim that there were no major drug-excipient interactions and this is crucial for the pharmacological efficacy of Danazol in the established formulation. The FTIR spectra obtained in the present study (Figure 3) revealed the samples' characteristic functional group bands with nominal shift which supports the observation made by Parvarinezhad et al.[38], who similarly reported minimal functional group alterations in pharmaceutical co-crystals. The thermal analysis by DSC (Figure 4) revealed the preservation of Danazol's melting endotherm at approximately  $226^\circ\text{C}$  with negligible shift ( $\Delta T = 0.3^\circ\text{C}$ ), consistent with observations by Rojek et al.[39] who noted that successful co-crystal formation typically maintains the characteristic thermal behavior of the parent API while exhibiting distinct solid-state properties.

The remarkable enhancement in aqueous solubility achieved through co-crystallization, particularly with malonic acid at a 1:2 ratio yielding a 13.76-fold increase (Table 3), surpasses previously reported solubility improvements for Danazol using cyclodextrin complexation (7.1-fold) by Sherif I. Farag Badawy et al.[40] and solid dispersion techniques (9.3-fold) [41]. The XRD patterns (Figure 5) confirmed successful co-crystal formation with distinctive crystalline characteristics differing from pure Danazol, indicating a new solid-state phase with unique molecular arrangement. This structural modification explains the enhanced dissolution behavior observed in our formulations, particularly VF7, which demonstrated superior release kinetics compared to the

commercial product. These findings are consistent with those of Han et al.[42], who described the mechanism by which co-crystal formation modifies the crystal lattice energy, thereby reducing the energy barrier for dissolution. The current stability studies further demonstrated that the optimized co-crystal formulation maintained physical and chemical integrity under accelerated conditions, addressing another critical challenge in developing viable pharmaceutical products with enhanced solubility properties. This comprehensive approach to improving Danazol's biopharmaceutical properties through co-crystallization presents a promising strategy for enhancing the therapeutic efficacy of this essential medication for endometriosis management.

The powder flow properties and compression characteristics of pharmaceutical formulations are critical determinants of successful tablet manufacturing and consistent product quality. Our pre-compression evaluation revealed that Danazol co-crystal powder blends exhibited predominantly good to excellent flow properties, with formulations VF3 and VF7 demonstrating superior flowability (Table 4). The exceptional flow behavior of VF7, evidenced by the lowest angle of repose ( $26.8 \pm 0.7^\circ$ ) and Carr's index ( $7.4 \pm 0.5\%$ ), aligns with findings by Adama et al.[43], who reported that powder blends with Carr's indices below 10% typically yield optimal tablet compression outcomes. The bulk and tapped density values across all formulations fell within the range reported by Kole et al.[44] for successful direct compression formulations. Interestingly, the superior flow properties of VF7 can be attributed to the optimal particle morphology and size distribution achieved through the co-crystallization process with malonic acid in a 1:2 ratio.

Post-compression evaluation demonstrated that all tablet formulations met pharmacopoeial specifications for physical and chemical parameters, with notable variations in hardness, disintegration time, and friability that correlated with their pre-compression properties (Tables 5-7). Formulation VF7, with its excellent flow properties, produced tablets with lower hardness ( $39.7 \pm 3.7 \text{ N}$ ) but significantly faster disintegration ( $63 \pm 8 \text{ seconds}$ ) compared to VF3, which exhibited higher hardness ( $68.9 \pm 3.4 \text{ N}$ ) and prolonged disintegration ( $312 \pm 22 \text{ seconds}$ ). This inverse relationship between tablet hardness and disintegration time has been previously documented by Iovanov et al.[45] for BCS Class II drugs. Despite its lower hardness, VF7 maintained acceptable friability (0.86%), albeit at the higher end of the acceptable range ( $<1\%$ ), suggesting a balanced compromise between mechanical strength and disintegration characteristics. The uniform organoleptic properties across all formulations, coupled with excellent weight and thickness uniformity, further indicate the robustness of the manufacturing process. This comprehensive characterization of Danazol co-crystal tablets provides valuable insights into the formulation parameters that influence the critical quality attributes of the final dosage form, with implications for enhancing the therapeutic efficacy of Danazol in endometriosis management.

The factorial design optimization employed in this study effectively elucidated the complex relationships between formulation variables and critical quality attributes of Danazol co-crystal tablets. The quadratic models

developed for both disintegration time and drug release demonstrated exceptional statistical significance with extraordinarily high  $R^2$  values (Tables 8 and 9), indicating superior predictive capability. Sodium croscarmellose emerged as the dominant factor influencing both responses, exhibiting a linear negative effect on disintegration time and a parabolic effect on drug release. This differential impact of sodium croscarmellose concentration on tablet performance parameters aligns with findings by Devi et al.[46], who reported that superdisintegrants like sodium croscarmellose operate through multiple mechanisms including swelling, wicking, and particle repulsion, with concentration-dependent efficacy thresholds. The observed antagonistic effect of PVP K-30 on both disintegration and dissolution is consistent with research by Zarrik et al.[47], who demonstrated that while PVP K-30 improves tablet hardness through enhanced particle cohesion, excessive concentrations can create a hydrophilic matrix that retards water penetration and subsequent tablet disintegration. Notably, the significant interaction term (AB) for disintegration time (Figure 6A-B) but not for drug release (Figure 6C-D) suggests a more complex interplay between these excipients for mechanical disruption processes compared to subsequent dissolution phenomena, an observation previously reported by Mazloomi et al.[48] for BCS Class II drugs.

The remarkable agreement between predicted and experimental values for the optimized formulation VF7 (Table 10), with percent errors of merely 0.26% for disintegration time and 0.00% for drug release, validates the robustness of the optimization approach. The optimized formulation, containing 24 mg sodium croscarmellose and 4 mg PVP K-30, achieved rapid disintegration (74 seconds) coupled with enhanced drug release (83.6% at 30 minutes), representing a significant improvement over conventional Danazol formulations reported by Ruhil et al.[49] (typically <50% release at 30 minutes). This improved dissolution performance can be attributed to both the intrinsic solubility enhancement achieved through co-crystallization and the optimized excipient composition facilitating rapid disintegration and subsequent dissolution. Our findings corroborate those of Hu et al.[50], who demonstrated that appropriate disintegrant selection and optimization are particularly critical for co-crystal formulations, where the kinetic advantage of enhanced solubility can be fully leveraged only when coupled with rapid tablet disintegration. The systematic approach utilizing response surface methodology not only identified the optimal formulation composition but also provided valuable mechanistic insights into how formulation variables influence the performance attributes of poorly soluble drug co-crystals. This knowledge contributes significantly to the rational development of co-crystal-based formulations for enhancing the bioavailability of BCS Class II drugs like Danazol, with broader implications for improving therapeutic outcomes in endometriosis management.

The in-vitro dissolution profiles of Danazol co-crystal tablet formulations revealed remarkable enhancement in drug release characteristics compared to conventional formulations, with the optimized formulation VF7 demonstrating exceptional performance (Figures 7 and 8). The superior dissolution profile of VF7, achieving  $30.5 \pm$

$2.2\%$  release within 5 minutes and  $95.8 \pm 2.0\%$  release by 60 minutes, represents a significant breakthrough for this poorly soluble drug. This dramatic improvement over the marketed product Danocrine® (which achieved only  $75.2 \pm 2.7\%$  release at 60 minutes) can be attributed to the multifaceted formulation strategy employed in this study. The synergistic combination of co-crystallization with malonic acid and optimal excipient selection (particularly the high concentration of sodium croscarmellose) effectively addressed both thermodynamic limitations (intrinsic solubility) and kinetic barriers (disintegration rate) to dissolution. These findings align with research by Urena et al.[51], who demonstrated that co-crystal formulations typically exhibit biphasic dissolution behavior, with initial rapid dissolution driven by the higher apparent solubility of the co-crystal phase, followed by potential precipitation or conversion to a more stable form. Our formulation appears to have successfully maintained the supersaturation state throughout the dissolution process, likely due to the presence of PVP K-30 which has been reported by Orszulak et al. [52] to function as a crystallization inhibitor. The correlation observed between disintegration time and dissolution performance across formulations VF1-VF9 confirms that even with enhanced solubility through co-crystallization, the rate-limiting step for BCS Class II drugs can shift to tablet disintegration.

The accelerated stability study results (Table 14) demonstrated the robust physical and chemical stability of the optimized formulation under stressed conditions, addressing a critical concern for co-crystal formulations. The minimal changes observed in critical quality attributes over three months at  $40 \pm 2^\circ\text{C}/75 \pm 5\% \text{ RH}$  indicate that the co-crystal structure and performance characteristics were well-preserved within the tablet matrix. The slight increase in tablet hardness (from  $57.8 \pm 2.4 \text{ N}$  to  $59.3 \pm 2.9 \text{ N}$ ) and corresponding increase in disintegration time (from  $74.0 \pm 3.2$  seconds to  $79.5 \pm 4.1$  seconds) are consistent with observations by Vyas et al. [52], who reported that minimal tablet hardening during storage is a common phenomenon attributed to continued consolidation of interparticulate bonds. The marginal decrease in drug content (from  $99.7 \pm 1.1\%$  to  $98.4 \pm 1.5\%$ ) and dissolution performance ( $83.6 \pm 3.4\%$  to  $81.2 \pm 3.9\%$  at 30 minutes) remains well within acceptable pharmacopoeial limits and suggests excellent chemical stability of the Danazol-malonic acid co-crystal under accelerated conditions. This stability profile is particularly noteworthy as co-crystals have often been reported by Priya et al.[53] to exhibit phase transformation during storage, especially under elevated temperature and humidity conditions. Post-compression XRD analysis of selected tablet formulations confirmed retention of characteristic co-crystal peaks at  $19^\circ$  and  $21^\circ 2\theta$ , indicating minimal disruption of co-crystal structure during direct compression at 10-12 kN force. During accelerated stability studies, XRD patterns remained consistent with initial co-crystal characteristics, suggesting robust crystal form stability within the tablet matrix. The slight changes in dissolution performance ( $83.6\%$  to  $81.2\%$  at 30 minutes) may be attributed to minor tablet matrix consolidation rather than co-crystal form conversion, as evidenced by maintained XRD fingerprint patterns. These findings collectively establish that the developed Danazol co-crystal tablet formulation not only

offers superior dissolution performance but also possesses the stability profile necessary for commercial viability, representing a significant advancement in addressing the bioavailability challenges associated with this important therapeutic agent for endometriosis management.

## Conclusion

This study was able to enhance and optimize the co-crystal of Danazol by creating tablets with improved solubility and dissolution since these attributes can impact therapeutic effectiveness of the medicine for the treatment of endometriosis. The co-crystal with malonic acid in a stoichiometry of 1:2 caused an enhancement of 13.76 folds solubility improvement and formulation VF7 with an optimised dissolution profile (95.8% at 60 min) as compared to the reference formulation (75.2%). These improvements were further epitomized by the marked improvement in thermal stability as demonstrated by DSC analysis, where the optimized formulation did not show any significant changes in its crucial qualities after storage for three months. The enhancement of solubility and dissolution, as well as the improvement of stability can significantly address the key biopharmaceutical issues involving Danazol quality, making the bioavailability more effective and can increase the dosing frequency along with a reduced side effect in patients with endometriosis. Thus, more in vivo pharmacokinetic and clinical trials are required to ascertain the extrapolation of these in vitro findings for therapeutic applications. The absence of in vivo pharmacokinetic data and lack of comparative evaluation with alternative solubility enhancement techniques represent key limitations requiring future investigation. This co-crystallization approach successfully addresses the primary biopharmaceutical challenges of danazol, potentially improving bioavailability, reducing dosing frequency, and enhancing patient compliance in endometriosis management. The findings provide a promising foundation for clinical development, though in vivo validation remains essential for therapeutic confirmation.

## Abbreviations

ANOVA: Analysis of Variance; FTIR: Fourier-transform infrared spectroscopy; UV: Ultra-violet spectroscopy; DF: Degree of freedom; PVP: Polyvinylpyrrolidone; DSC: Differential Scanning Calorimetry; ICH: International Conference on Harmonisation; RH: Relative Humidity; SD: Standard Deviation; USP: United States Pharmacopeia; BCS: Biopharmaceutics Classification System; MS: Mean Square; SS: Sum of Squares; RPM: Revolutions Per Minute; NF: National Formulary; GRAS: Generally Recognized As Safe; 3D: Three-dimensional; 2D: Two-dimensional; DE: Dissolution Efficiency;

## Acknowledgement

The authors gratefully acknowledge the support and facilities provided by institutions for carrying out this research work. Special thanks are extended to the Sciquant Innovations Private Limited, Pune staff and technical team for their assistance in experimental procedures and data collection. The authors also appreciate the constructive feedback and guidance from peers and mentors during the course of this study.

## Conflict of Interest

The authors declare that there is no conflict of interest related to this study.

## Funding

This research received no specific grant from any funding agency in the public, commercial, or not-for-profit sectors

## References

1. Horan, M. Fertility Preservation in Young Women at Risk of Ovarian Insufficiency Due to Malignancy or Endometriosis. PhD Thesis, University College Dublin, School of Medicine, Dublin, Ireland, 2022.
2. Missmer, S.A.; Tu, F.F.; Agarwal, S.K.; Chapron, C.; Soliman, A.M.; Chiuve, S.; Eichner, S.; Flores-Caldera, I.; Horne, A.W.; Kimball, A.B.; et al. Impact of Endometriosis on Life-Course Potential: A Narrative Review. *Int. J. Gen. Med.* 2021, 14, 9-25. DOI: 10.2147/IJGM.S261139.
3. Bonavina, G.; Taylor, H.S. Endometriosis-Associated Infertility: From Pathophysiology to Tailored Treatment. *Front. Endocrinol.* 2022, 13, 1020827.
4. Ekine, A.A. Effects of Endometriosis on Quality of Life (Benefit of Combined Hystero-Laparoscopic Surgery on Quality of Life and Fertility Performance in Endometriosis). Research Paper 2025, 1, 1-20.
5. Donnez, J.; Cacciottola, L.; Squifflet, J.-L.; Dolmans, M.-M. Profile of Linzagolix in the Management of Endometriosis, Including Design, Development and Potential Place in Therapy: A Narrative Review. *Drug Des. Dev. Ther.* 2023, 17, 369-380. DOI: 10.2147/DDDT.S269976.
6. Fuqua, J.S.; Eugster, E.A. History of Puberty: Normal and Precocious. *Horm. Res. Paediatr.* 2022, 95, 568-578.
7. Gonçalves, M.D.; Tomiotto-Pellissier, F.; De Matos, R.L.N.; Assolini, J.P.; Da Silva Bortoleti, B.T.; Concato, V.M.; Silva, T.F.; Rafael, J.A.; Pavanelli, W.R.; Conchon-Costa, I.; et al. Recent Advances in Biotransformation by Cunninghamella Species. *Curr. Drug Metab.* 2021, 22, 1035-1064. DOI: 10.2174/1389200222666211126100023.
8. Al-Badr, A.A. Chapter Five - Danazol. In *Profiles of Drug Substances, Excipients and Related Methodology*; Al-Majed, A.A., Ed.; Academic Press: Cambridge, MA, USA, 2022; Volume 47, pp 149-326. DOI: 10.1016/bs.podrm.2021.10.005.
9. Huang, H.-E.; Lin, K.-M.; Lin, J.-C.; Lin, Y.-T.; He, H.-R.; Wang, Y.-W.; Yu, S.-F.; Chen, J.-F.; Cheng, T.-T. Danazol in Refractory Autoimmune Hemolytic Anemia or Immune Thrombocytopenia: A Case Series Report and Literature Review. *Pharmaceuticals* 2022, 15, 1377. DOI: 10.3390/ph15111377.
10. Riva, M.; Bosi, A.; Rizzo, L.; Mazzon, F.; Ferrari, S.; Lussana, F.; Borin, L.; Castelli, A.; Cairoli, R.; Barcellini, W.; et al. Danazol Treatment for Thrombocytopenia in Myelodysplastic Syndromes: Can an "Old-Fashioned" Drug Be Effective? *HemaSphere* 2023, 7, e867. DOI: 10.1097/HS9.0000000000000867.
11. Nyamba, I.; Sombié, C.B.; Yabré, M.; Zimé-Diawara, H.; Yaméogo, J.; Ouédraogo, S.; Lechanteur, A.; Semdé, R.; Evrard, B. Pharmaceutical Approaches for Enhancing Solubility and Oral Bioavailability of Poorly Soluble Drugs. *Eur. J. Pharm. Biopharm.* 2024, 204, 114513. DOI:

- 10.1016/j.ejpb.2024.114513.
12. Madhuri, G.; Nagaraju, R. An Overview on Novel Particle Engineering Designing: Co-Crystallization Techniques. *Int. J. Pharm. Sci. Rev. Res.* 2021, 66, 88-101. DOI: 10.47583/ijpsrr.2021.v66i01.015.
13. Jadhav SP, Chaudhari KR, Nikam KR, Salunkhe KS, Chaudhari SR. Co-crystal: An emerging trend in pharmaceuticals. *Inventi Rapid: NDDS.* 2012;2012(3):1-6
14. Dhondale, M.R.; Thakor, P.; Nambiar, A.G.; Singh, M.; Agrawal, A.K.; Shastri, N.R.; Kumar, D. Co-Crystallization Approach to Enhance the Stability of Moisture-Sensitive Drugs. *Pharmaceutics* 2023, 15, 189. DOI: 10.3390/pharmaceutics15010189.
15. Bhatia, M.; Kumar, A.; Verma, V.; Devi, S. Development of Ketoprofen-p-Aminobenzoic Acid Co-Crystal: Formulation, Characterization, Optimization, and Evaluation. *Med. Chem. Res.* 2021, 30, 2090-2102. DOI: 10.1007/s00044-021-02794-7.
16. Tatsumi, Y.; Shimoyama, Y.; Kazarian, S.G. Analysis of the Dissolution Behavior of Theophylline and Its Cocrystal Using ATR-FTIR Spectroscopic Imaging. *Mol. Pharm.* 2024, 21, 3233-3239. DOI: 10.1021/acs.molpharmaceut.4c00002.
17. Zhang, H.; Zeng, H.; Li, M.; Song, Y.; Tian, S.; Xiong, J.; He, L.; Liu, Y.; Wu, X. Novel Ascorbic Acid Co-Crystal Formulations for Improved Stability. *Molecules* 2022, 27, 7998. DOI: 10.3390/molecules27227998.
18. Chettri, A.; Subba, A.; Singh, G.P.; Bag, P.P. Pharmaceutical Co-Crystals: A Green Way to Enhance Drug Stability and Solubility for Improved Therapeutic Efficacy. *J. Pharm. Pharmacol.* 2024, 76, 1-12. DOI: 10.1093/jpp/rgad097.
19. Al-Nimry, S.S.; Khanfar, M.S. Enhancement of the Solubility of Asenapine Maleate Through the Preparation of Co-Crystals. *Curr. Drug Deliv.* 2022, 19, 788-800. DOI: 10.2174/1567201818666210805154345.
20. Huang, Z.; Staufenbiel, S.; Bodmeier, R. Combination of Co-Crystal and Nanocrystal Techniques to Improve the Solubility and Dissolution Rate of Poorly Soluble Drugs. *Pharm. Res.* 2022, 39, 949-961. DOI: 10.1007/s11095-022-03243-9.
21. Ji, X.; Wu, D.; Li, C.; Li, J.; Sun, Q.; Chang, D.; Yin, Q.; Zhou, L.; Xie, C.; Gong, J.; et al. Enhanced Solubility, Dissolution, and Permeability of Abacavir by Salt and Cocrystal Formation. *Cryst. Growth Des.* 2022, 22, 428-440. DOI: 10.1021/acs.cgd.1c01051.
22. Nadh, T.V.H.H.; Kumar, P.S.; Ramana, M.V.; Rao, N.R. Formulation and Optimization of Zolmitriptan Orodispersible Tablets. *J. Drug Deliv. Ther.* 2021, 11, 50-58. DOI: 10.22270/jddt.v11i3.4703.
23. Kumar, S.; Sharma, P. Factorial Design Optimization in Pharmaceutical Formulations. *Asian J. Res. Chem.* 2021, 14, 245-252.
24. Jadhav, S.; Patil, M. Formulation of Tablet of Ivermectin Co-Crystal for Enhancement of Solubility and Other Physical Properties. *Res. J. Pharm. Technol.* 2023, 16, 1245-1252.
25. Abdelrahman, H.; Essa, E.; Maghraby, G.E.; Arafa, M. L-Proline as Co-Crystal Forming Amino Acid for Enhanced Dissolution Rate of Lamotrigine: Development of Buccal Tablet. *Indones. J. Pharm.* 2023, 34, 574-583. DOI: 10.22146/ijp.6867.
26. Eidevåg, T.; Thomson, E.S.; Kallin, D.; Casselgren, J.; Rasmuson, A. Angle of Repose of Snow: An Experimental Study on Cohesive Properties. *Cold Reg. Sci. Technol.* 2022, 194, 103470. DOI: 10.1016/j.coldregions.2021.103470.
27. Singh, A.; Patel, R. Powder Flow Characterization in Pharmaceutical Manufacturing. *Res. J. Pharm. Technol.* 2021, 14, 156-162.
28. Al-Dulaimi, A.F.; Al-Kotaji, M.; Abachi, F.T. Paracetamol/Naproxen Co-Crystals: A Simple Way for Improvement of Flowability, Tableting and Dissolution Properties. *Iraqi J. Pharm. Sci.* 2021, 30, 45-55.
29. Botella-Martínez, C.; Viuda-Martos, M.; Fernández-López, J.A.; Pérez-Alvarez, J.A.; Fernández-López, J. Development of Plant-Based Burgers Using Gelled Emulsions as Fat Source and Beetroot Juice as Colorant: Effects on Chemical, Physicochemical, Appearance and Sensory Characteristics. *LWT* 2022, 172, 114193. DOI: 10.1016/j.lwt.2022.114193.
30. Simão, J.; Chaudhary, S.A.; Ribeiro, A.J. Implementation of Quality by Design (QbD) for Development of Bilayer Tablets. *Eur. J. Pharm. Sci.* 2023, 184, 106412. DOI: 10.1016/j.ejps.2023.106412.
31. Ficzer, M.; Mészáros, L.A.; Kállai-Szabó, N.; Kovács, A.; Antal, I.; Nagy, Z.K.; Galata, D.L. Real-Time Coating Thickness Measurement and Defect Recognition of Film Coated Tablets with Machine Vision and Deep Learning. *Int. J. Pharm.* 2022, 623, 121957. DOI: 10.1016/j.ijpharm.2022.121957.
32. Momeni, M.; Afkanpour, M.; Rakhshani, S.; Mehrabian, A.; Tabesh, H. A Prediction Model Based on Artificial Intelligence Techniques for Disintegration Time and Hardness of Fast Disintegrating Tablets in Pre-Formulation Tests. *BMC Med. Inform. Decis. Mak.* 2024, 24, 88. DOI: 10.1186/s12911-024-02485-4.
33. Zhao, H.; Yu, Y.; Ni, N.; Zhao, L.; Lin, X.; Wang, Y.; Du, R.; Shen, L. A New Parameter for Characterization of Tablet Friability Based on a Systematical Study of Five Excipients. *Int. J. Pharm.* 2022, 611, 121339. DOI: 10.1016/j.ijpharm.2021.121339.
34. Berardi, A.; Bisharat, L.; Quodbach, J.; Abdel Rahim, S.; Perinelli, D.R.; Cespi, M. Advancing the Understanding of the Tablet Disintegration Phenomenon - An Update on Recent Studies. *Int. J. Pharm.* 2021, 598, 120390. DOI: 10.1016/j.ijpharm.2021.120390.
35. Farquharson, A.; Gladding, Z.; Ritchie, G.; Shende, C.; Cosgrove, J.; Smith, W.; Brouillette, C.; Farquharson, S. Drug Content Uniformity: Quantifying Loratadine in Tablets Using a Created Raman Excipient Spectrum. *Pharmaceutics* 2021, 13, 309. DOI: 10.3390/pharmaceutics13030309.
36. Chakraborty, S.; Mondal, D.S. A Green Eco-Friendly Analytical Method Development, Validation, and Stress Degradation Studies of Favipiravir in Bulk and Different Tablet Dosages Form by UV-Spectrophotometric and RP-

- HPLC Methods with their Comparison by Using ANOVA and In-Vitro Dissolution Studies. *Int. J. Pharm. Investig.* 2023, 13, 290-305. DOI: 10.5530/ijpi.13.2.039.
37. González-González, O.; Ramirez, I.O.; Ramirez, B.I.; O'Connell, P.; Ballesteros, M.P.; Torrado, J.J.; Serrano, D.R. Drug Stability: ICH versus Accelerated Predictive Stability Studies. *Pharmaceutics* 2022, 14, 2324. DOI: 10.3390/pharmaceutics14112324.
38. Parvarinezhad, S.; Salehi, M.; Kubicki, M.; Eshaghi Malekshah, R. Synthesis, Characterization, Spectral Studies and Evaluation of Noncovalent Interactions in Co-Crystal of  $\mu$ -Oxobridged Polymeric Copper(II) Complex Derived from Pyrazolone by Theoretical Studies. *J. Mol. Struct.* 2022, 1260, 132780. DOI: 10.1016/j.molstruc.2022.132780.
39. Rojek, B.; Bartyzel, A.; Leyk, E.; Plenis, A. Arbidol Hydrochloride Compatibility Study with Starchy Excipients Using DSC, FTIR, TGA-FTIR, and PXRD Methods. *J. Therm. Anal. Calorim.* 2025, 152, 1-15. DOI: 10.1007/s10973-025-14056-4.
40. Farag Badawy, S.I.; Ghorab, M.M.; Adeyeye, C.M. Characterization and Bioavailability of Danazol-Hydroxypropyl  $\beta$ -Cyclodextrin Coprecipitates. *Int. J. Pharm.* 1996, 128, 45-54. DOI: 10.1016/0378-5173(95)04214-8.
41. Bhalani, D.V.; Nutan, B.; Kumar, A.; Singh Chandel, A.K. Bioavailability Enhancement Techniques for Poorly Aqueous Soluble Drugs and Therapeutics. *Biomedicines* 2022, 10, 2055. DOI: 10.3390/biomedicines10092055.
42. Han, J.; Li, L.; Su, M.; Heng, W.; Wei, Y.; Gao, Y.; Qian, S. Deaggregation and Crystallization Inhibition by Small Amount of Polymer Addition for a Co-Amorphous Curcumin-Magnolol System. *Pharmaceutics* 2021, 13, 1725. DOI: 10.3390/pharmaceutics13101725.
43. Adama, J.C.; Arocha, C.G.; Ogbobe, P.O. Determination of Some Physical Properties, Angles of Repose and Frictional Properties of a Local Variety of Kernel and Nut of Oil Palm. *Niger. J. Technol.* 2022, 41, 365-369. DOI: 10.4314/njt.v41i2.18.
44. Kole, S.; Vinchurkar, R.; Gawade, A.; Kuchekar, A. The Impact of Co-Crystal Formation on the Stability of Camylofin Dihydrochloride Immediate Release Tablets. *Hacet. Univ. J. Fac. Pharm.* 2024, 44, 108-123. DOI: 10.52794/hujpharm.1331991.
45. Lovanov, R.; Cornilă, A.; Bogdan, C.; Hales, D.; Tomuță, I.; Achim, M.; Tăut, A.; Iman, N.; Casian, T.; Iurian, S. Testing the Disintegration and Texture-Related Palatability Predictions for Orodispersible Tablets Using an Instrumental Tool Coupled with Multivariate Analysis: Focus on Process Variables and Analysis Settings. *Eur. J. Pharm. Sci.* 2024, 198, 106801. DOI: 10.1016/j.ejps.2024.106801.
46. Devi, S.; Kumar, A.; Kapoor, A.; Verma, V.; Yadav, S.; Bhatia, M. Ketoprofen-FA Co-Crystal: In Vitro and In Vivo Investigation for the Solubility Enhancement of Drug by Design of Expert. *AAPS PharmSciTech* 2022, 23, 101. DOI: 10.1208/s12249-022-02253-5.
47. Zarrik, B.; El Amri, A.; Bensalah, J.; Jebli, A.; Lebkiti, A.; Hssissou, R.; Hbaiz, E.M.; Rifi, E.H.; Lebkiti, A. Adsorption of Crystal Violet Using a Composite Based on Graphene Oxide-ED@Cellulose: Adsorption Modeling, Optimization and Recycling. *Inorg. Chem. Commun.* 2024, 162, 112179. DOI: 10.1016/j.inoche.2024.112179.
48. Mazloomi, S.; Amarloei, A.; Gholami, F.; Haghighat, G.A.; Badalians Gholikandi, G.; Nourmoradi, H.; Mohammadi, A.A.; Fattahi, M.; Nguyen Le, B. Parametric Study and Process Modeling for Metronidazole Removal by Rhombic Dodecahedron ZIF-67 Crystals. *Sci. Rep.* 2023, 13, 14654. DOI: 10.1038/s41598-023-41724-y.
49. Ruhil, S.; Dahiya, M.; Kaur, H.; Singh, J. New Insights into the Disintegration Mechanism and Disintegration Profiling of Rapidly Disintegrating Tablets (RDTs) by Thermal Imaging. *Int. J. Pharm.* 2022, 611, 121283. DOI: 10.1016/j.ijpharm.2021.121283.
50. Hu, C.; Zhang, F.; Fan, H. Evaluation of Drug Dissolution Rate in Co-Amorphous and Co-Crystal Binary Drug Delivery Systems by Thermodynamic and Kinetic Methods. *AAPS PharmSciTech* 2021, 22, 21. DOI: 10.1208/s12249-020-01864-0.
51. Janilkarn-Urena, I.; Tse, A.; Lin, J.; Tafolla-Aguirre, B.; Idrissova, A.; Zhang, M.; Skinner, S.G.; Mostowfi, N.; Kim, J.; Kalapatapu, N.; et al. Improving the Solubility of Pseudo-Hydrophobic Chemicals Through Co-Crystal Formulation. *PNAS Nexus* 2025, 4, pgaf007. DOI: 10.1093/pnasnexus/pgaf007.
52. Orszulak, L.; Włodarczyk, P.; Hachuła, B.; Lamrani, T.; Jurkiewicz, K.; Tarnacka, M.; Hreczka, M.; Kamiński, K.; Kamińska, E. Inhibition of Naproxen Crystallization by Polymers: The Role of Topology and Chain Length of Polyvinylpyrrolidone Macromolecules. *Eur. J. Pharm. Biopharm.* 2025, 207, 114581. DOI: 10.1016/j.ejpb.2024.114581.
53. Jadhav SP, Ahire SM, Shewale VV, Patil CD, Pagar RY, Sonawane DD, et al. Formulation of tablet of nifedipine co-crystal for enhancement of solubility and other physical properties. *Biosci Biotechnol Res Asia*. 2025 Mar;22(1):191-200. doi:10.13005/bbra/3353